



ELSEVIER

1 August 1999

OPTICS
COMMUNICATIONS

Optics Communications 166 (1999) 95–102

www.elsevier.com/locate/optcom

Temporal and spectral characteristics of an additive-pulse mode-locked Nd:YLF laser with Michelson-type configuration

T.M. Jeong, E.C. Kang, C.H. Nam *

Department of Physics, Korea Advanced Institute of Science and Technology, 373-1, Kusong-dong, Yuseong-gu, Taejeon 305-701, South Korea

Received 10 March 1999; received in revised form 13 May 1999; accepted 19 May 1999

Abstract

The temporal and spectral characteristics of a laser diode-pumped, additive-pulse mode-locked Nd:YLF laser have been investigated with respect to the cavity detuning between main and external cavities. In the case of a usual output through the beam splitter between main and external cavities, a strong temporal modulation was observed from an intensity autocorrelation trace which was also confirmed by a calculation based on intensity-dependent reflectance. To obtain mode-locked pulses without any temporal modulation, an output was directly extracted from the main cavity, and clean pulses with 1.7 ps duration were obtained at 1053 nm. © 1999 Published by Elsevier Science B.V. All rights reserved.

Keywords: Additive-pulse mode-locking; Temporal modulation; Laser diode pumping; Michelson-type configuration; Nd:YLF

1. Introduction

New passive mode-locking techniques, such as additive-pulse mode-locking (APM) [1] and Kerr-lens mode-locking (KLM) [2] which utilize a non-linear Kerr effect, have been recently developed and could generate stable, ultrashort pulses in the picosecond or femtosecond range. An APM laser can be rather easily realized, in comparison to an KLM laser, by adding a non-linear element, such as a single mode fiber. Due to relatively easy generation of mode-locked pulses, APM has been applied to a number of solid-state lasers, such as Nd:YAG [3], Nd:YLF [4] and Nd:glass [5], and its properties such as pulse width, self-starting [6], and repetition rate [7] were

widely investigated. The combination of APM technique with laser diode (LD) pumping could realize a highly efficient, compact and stable all solid-state laser.

As a kind of the coupled-cavity mode-locking (CCM) [8,9] with two cavities, APM has an acceptable cavity detuning range to generate mode-locked pulses. This cavity detuning range can be divided into two groups: the fine cavity detuning within the range of wavelength due to the interferometric nature of the APM process and the coarse cavity detuning in the range of a few hundreds μm to a few millimeters approximately corresponding to the pulse duration. Although APM can be easily realized by using a single mode fiber, it needs a stabilization unit to maintain mode-locking within the fine cavity detuning range. Since the development of the stable, solid-state, and ultrashort APM laser, the temporal

* Corresponding author. Fax: 82-42-869-2510; e-mail: chnam@sorak.kaist.ac.kr

characteristics such as the pulse width and its dependence on the cavity detuning have been widely investigated theoretically and experimentally from the mode-locked pulse [8,10].

The output pulses of APM lasers, on the other hand, have the possibility of the temporal modulation due to the coupling of two cavities through an intensity-dependent reflectance. The temporal modulation of APM laser may cause a limitation to certain applications in which the temporal structure of a driving laser is critical. With the effort of the characterization of the temporal profile as well as the pulse width, Chee et al. [11] investigated the temporal and spectral shape from a flashlamp-pumped APM Nd:YLF laser pulse with respect to the cavity detuning and observed an asymmetric pulse profile from the output pulse. However, they investigated only the characteristics of pulses in the external cavity, and did not analyze pulses in the main cavity with respect to the coarse cavity detuning between main and external cavities.

In this paper, we analyzed the temporal and spectral properties of pulses in the main and the external cavities of an LD-pumped, APM Nd:YLF laser with respect to the coarse cavity detuning. The temporal and spectral characteristics of mode-locked pulses at various positions were analyzed and a method to generate clean and short pulse was proposed. By installing an output coupler in the main cavity, instead of utilizing the beam splitter between main and external cavities as the output coupler, pulses with 1.7 ps duration without any temporal modulation were obtained.

2. Pulse formation in additive-pulse mode-locking

The schematic diagram of an APM laser which consists of main and external cavities in a Michelson-type configuration is shown in Fig. 1a. The amplitudes of incident and returning electric fields at the beam splitter (BS) are represented as a_1 and b_1 in the main cavity and a_2 and b_2 in the external cavity, respectively. These amplitudes are related by

$$b_1(t) = r^2 a_1(t) + \sqrt{1-r^2} a_2(t), \quad (1)$$

$$b_2(t) = \sqrt{1-r^2} a_1(t), \quad (2)$$

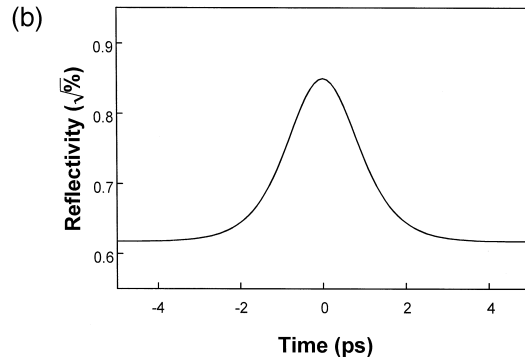
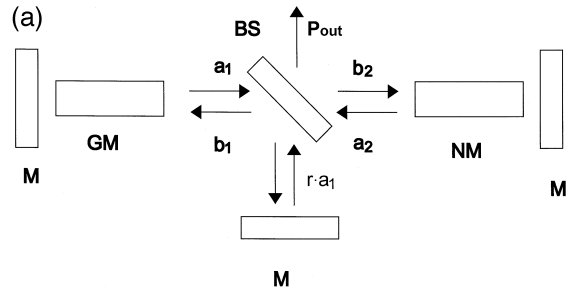


Fig. 1. (a) Schematic diagram of an additive-pulse mode-locked laser with a Michelson-type configuration. M, mirror; BS, beam splitter; GM, gain medium; NM, nonlinear medium. (b) Effective reflectance of a sech^2 pulse at the beam splitter (BS).

where r is the nominal reflectivity of BS. The amplitude $a_2(t)$ is given by

$$a_2(t) = L \cdot \exp(-j\{\phi + \Phi(t)\}) b_2(t), \quad (3)$$

with

$$\Phi(t) = \frac{2\pi n_2 I l}{\lambda} (|a_2(t)|^2 - |a_2(0)|^2), \quad (4)$$

where L is the coupling loss into the fiber, I the intensity in the non-linear medium, l the length of the non-linear medium, and n_2 the non-linear refractive index $5.8 \times 10^{-16} \text{ cm}^2/\text{W}$ for silicate glass. In Eq. (3), ϕ is the linear phase shift set by the difference in the two cavity lengths and $\Phi(t)$ is the non-linear phase shift induced in the non-linear medium. Then, the effective reflectivity, $\Gamma(t)$, at BS may be written as

$$\Gamma(t) \equiv \frac{b_1(t)}{a_1(t)} = r^2 + (1-r^2)L \cdot \exp\{-j(\phi + \Phi(t))\}. \quad (5)$$

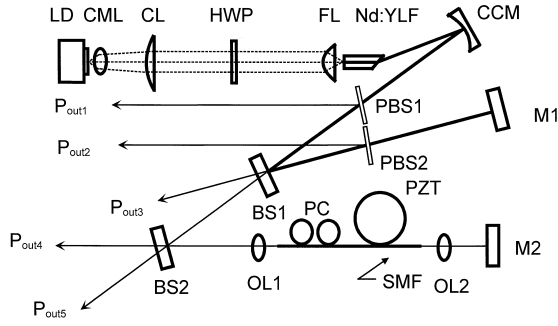


Fig. 2. Optical layout of an LD pumped, additive-pulse mode-locked Nd:YLF laser with Michelson-type configuration. LD, laser diode; HWP, half-wave plate; PBS1,2, pellicle beam splitter; BS1,2, beam splitter; PZT, piezoelectric transducer; SMF, single mode fiber; PC, polarization controller; M1,2, mirror; OL1,2, objective lens; CML, collimation lens; CL, cylindrical lens; FL, focusing lens; CCM, concave mirror.

This effective reflectivity is similar to the approximate representation ($L \ll 1$) of a Fabry–Perot-type configuration [12]. It shows that the beam splitter plays the role of an intensity-dependent mirror by which a higher intensity part is reflected more strongly. Fig. 1b shows the effective reflectance of a sech^2 pulse with 2 ps duration at the beam splitter. The nominal reflectance of the beam splitter and the fiber length were assumed 85% and 1.2 m, respectively, and the coupling loss L was taken as 0.74, considering the coupling efficiency into the fiber. Fig. 1b shows that the low-intensity part of the pulse experiences the low reflectance because of the destructive interference due to the self-phase modulation induced in the fiber.

On account of the characteristics of coupled cavity, the pulse returned from the external cavity may be preceded or delayed with respect to the pulse in the main cavity at the beam splitter because of the existence of cavity detuning. The output is usually taken from the beam splitter in the Michelson-type configuration as shown in Fig. 1a. Then, the output pulse P_{out} is the sum of pulses from the main cavity and the external cavity and may be represented after one round trip in steady-state condition as follows:

$$P_{\text{out}}(t) = r\sqrt{1 - \Gamma(t + \tau)^2} a_1(t) + L\sqrt{1 - r^2} \Gamma(t + \tau) a_1(t + \tau), \quad (6)$$

where τ is the time delay due to the coarse cavity detuning. In Eq. (6), the first term in the right-hand side is the transmitted pulse from the main cavity and the second term is the reflected one from the external cavity by BS with the effective non-linear reflectivity $\Gamma(t)$ given by Eq. (5). As the circulating power in the main cavity is usually greater than that in the external cavity and a beam splitter of 85% is used, the first term in Eq. (6) is greater than the second term. Thus, if the pulse through BS experiences the temporal modulation due to the effective reflectivity, the output pulse may also experience the temporal modulation. This temporal modulation due to the effective reflectivity is presented in Section 4 with respect to the coarse cavity detuning.

3. Laser configuration

The optical layout of an LD-pumped, APM Nd:YLF laser is shown in Fig. 2. The Nd:YLF laser was arranged in a Michelson-type configuration for the stable operation. The detailed feature of the Nd:YLF laser was described in our previous result [13]. The main cavity of the Nd:YLF laser was formed between the high reflecting flat surface of the laser rod and the mirror M1 through the beam splitter (BS1) with 85% reflectivity. The external cavity was formed between the flat surface of the rod and the end mirror M2 through the beam splitter (BS2)

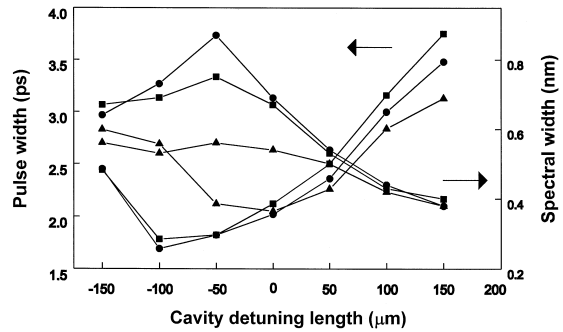


Fig. 3. Variation of the pulse width and spectral width with respect to the cavity detuning. Pulse width and spectral width of P_{out1} from PBS1 (circle), P_{out2} from PBS2 (square), and P_{out3} from BS1 (triangle).

with 98% reflectivity. The length of the external cavity was configured to have twice that of the main cavity. To maintain a stable mode-locking, an active stabilizer, similar to Mollenauer's [14], was used to match the phase of a pulse from the external cavity with that from the main cavity at the pulse peak. An

error signal was picked up from the beam splitter BS2 and fed back to the stabilizer.

The length of the external cavity could be adjusted by two steps: coarse and fine. The coarse cavity detuning was achieved by moving the mirror M2 installed on a translator. The mode-locking could

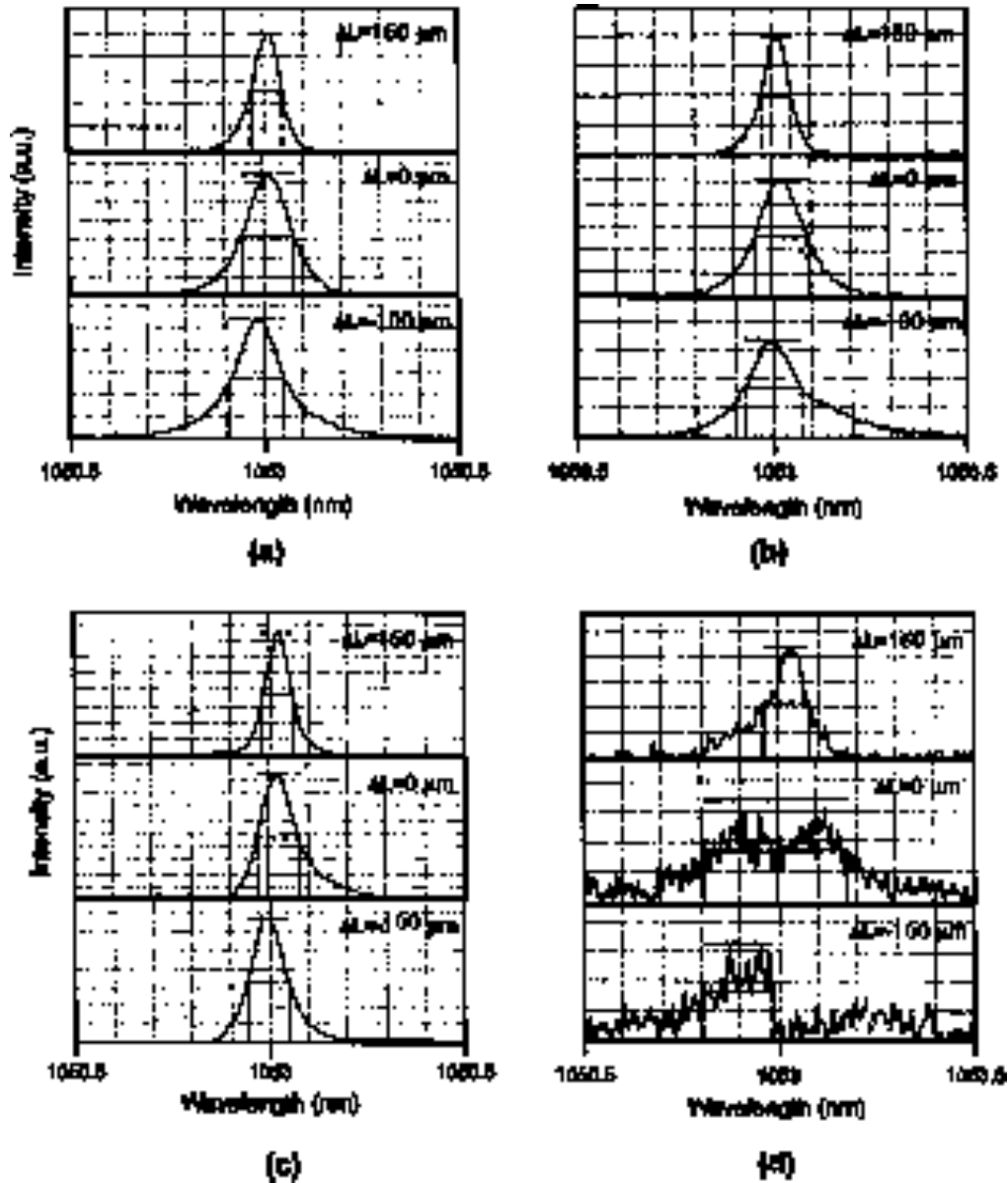


Fig. 4. Spectral profiles of an LD pumped, additive-pulse mode-locked Nd:YLF laser with respect to the cavity detuning length at four different positions. Spectral profiles of (a) P_{out1} , (b) P_{out2} , (c) P_{out3} , and (d) P_{out4} .

be maintained for the coarse cavity detuning of about 300 μm which roughly corresponded to the pulse width of 2 ps. The fine cavity tuning was achieved by controlling the length of the fiber wound on a cylindrical piezoelectric transducer (PZT). The shortest pulse width at each coarse cavity detuning was obtained by controlling the applied voltage to PZT within the fine cavity detuning range. To measure the pulse width and spectrum of the intracavity pulse at two positions in the main cavity, two pellicle beam splitters (PBS), PBS1 and PBS2, with the thickness of 10 μm were installed in the main cavity, before and after the beam splitter, respectively. The laser output was extracted at four positions. As in Fig. 2, $P_{\text{out}1}$ and $P_{\text{out}2}$ are the output from PBS1 and PBS2 installed in the main cavity. $P_{\text{out}3}$ through BS1 is the output usually used in most APM lasers. $P_{\text{out}4}$ and $P_{\text{out}5}$ through BS2 are used to

feed back to the active stabilizer and to monitor the mode-locked pulse train, respectively.

4. Temporal and spectral characteristics of the APM Nd:YLF laser

When the characteristics of only usual output through the beam splitter in APM are investigated, it is difficult to find the condition to generate the shortest and clean pulses from APM lasers. In order to understand the effect of the coarse cavity detuning on the temporal characteristics and to find out the shortest and clean pulse, the temporal and spectral widths need to be simultaneously measured at various location in the APM cavity. In our experiments, outputs at three positions ($P_{\text{out}1}$, $P_{\text{out}2}$, and $P_{\text{out}3}$, respectively) were monitored with respect to the

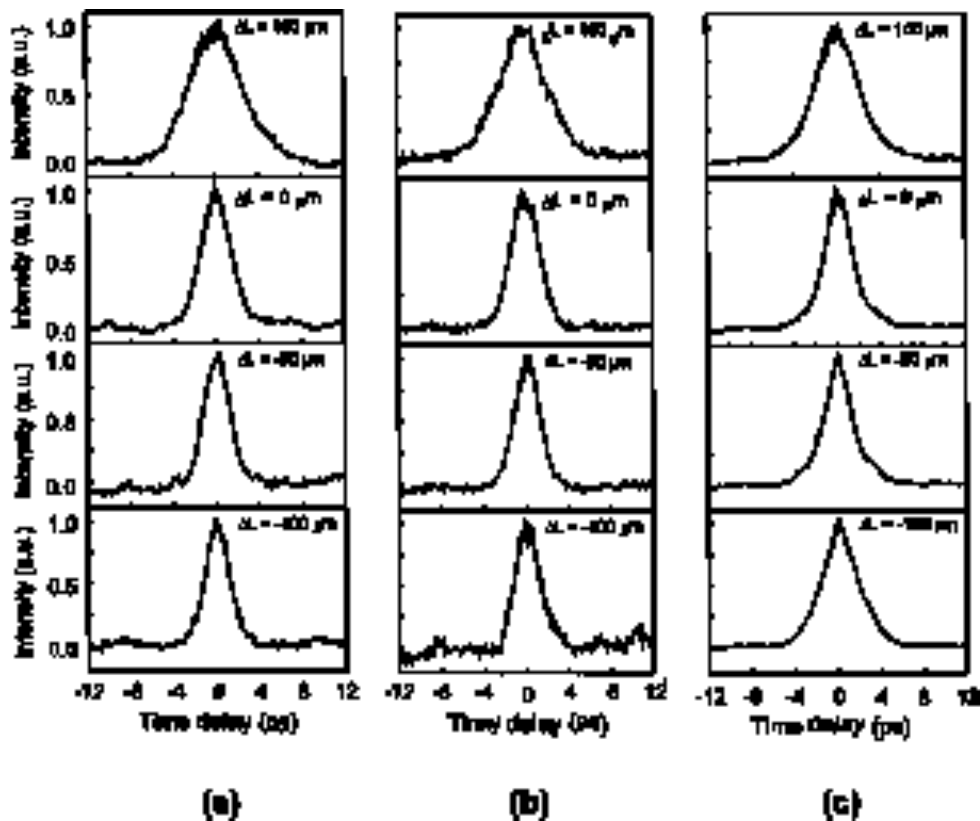


Fig. 5. Autocorrelation traces of an LD pumped, additive-pulse mode-locked Nd:YLF laser with respect to the cavity detuning length measured at three different positions. Autocorrelation traces of pulses from (a) $P_{\text{out}1}$, (b) $P_{\text{out}2}$, and (c) $P_{\text{out}3}$.

coarse cavity detuning in the APM Nd:YLF laser. The measured temporal and spectral widths are shown in Fig. 3. The coarse cavity detuning, ΔL , was defined by $\Delta L = l_e - l_m$, where l_e is the length of the external cavity and l_m the length of the main cavity. All the pulse widths varied similarly with respect to the coarse cavity detuning. The shortest pulse width of 1.7 ps and the broadest spectrum of 8.6 Å were obtained from $P_{\text{out}1}$. This result can be well explained by the calculation by Ippen et al. [16] which showed that the pulse incident into the gain medium is shortest. In our experiment, the positions generating the shortest pulse width and the broadest spectrum did not coincide. On the other hand, the pulse width and spectral width of $P_{\text{out}3}$ used as the usual output have a slightly broader pulse width of 2.1 ps and narrower spectrum of 6 Å. This spectral narrowing may come from the spectral filtering effect due to the interferometric addition at the beam splitter.

Since the output pulses of the APM laser have the possibility of the temporal modulation from Eq. (6), it is valuable to investigate the effect of the non-linear reflectance on the temporal and spectral profile due to the interferometric addition and the coarse cavity detuning. The autocorrelations and spectra were carefully observed for a detailed investigation. Fig. 4 shows the measured spectra of the APM Nd:YLF laser with respect to the coarse cavity detuning. The spectra were measured at four different positions ($P_{\text{out}1}$, $P_{\text{out}2}$, $P_{\text{out}3}$, and $P_{\text{out}4}$, respectively). The spectrum of the mode-locked pulse was measured with the optical spectrum analyzer with the resolution of 1 Å. Similarly to the observation by Chee et al. [11] for the case of a flashlamp-pumped APM Nd:YLF laser, all the peaks of the spectra slightly shifted to the short wavelength when shortening the length of the external cavity. When an optical pulse propagates in the optical fiber, the short wavelength component was delayed with respect to the long wavelength component because of the positive chirping due to SPM in the fiber. This delayed short wavelength component interferes with the pulse circulating in the main cavity when decreasing the external cavity length. As a result of this interference, the slight blue shift of the spectrum was observed with the negative cavity detuning. As shown in Fig. 4d, the spectrum of $P_{\text{out}4}$, spectrum of the

pulse returning from the optical fiber, had the broadest spectrum and showed the typical profile due to SPM in the fiber. When decreasing the external cavity length, it was observed that the long wavelength component disappeared. When the detuning position with the symmetric spectrum in Fig. 4a is assumed as the exact match of the cavity length, the shortest pulse was obtained in the negative cavity detuning in contrast to the earlier studies that the shortest pulse could be generated at the exact match of the cavity length [15].

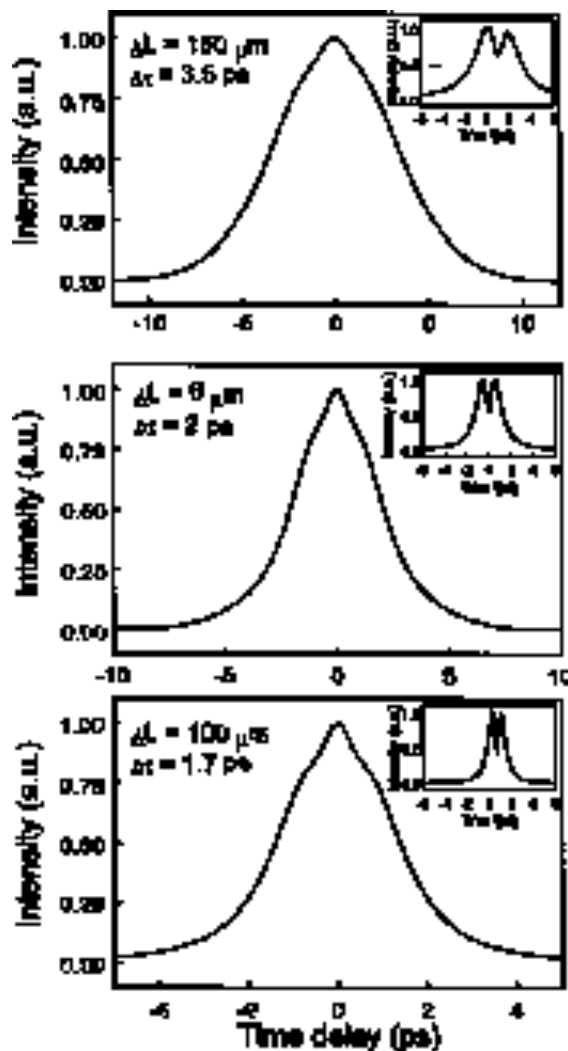


Fig. 6. Calculated temporal pulse shape and its autocorrelation trace with respect to the cavity detuning.

Fig. 5 shows the intensity autocorrelation traces with respect to the coarse cavity detuning measured at three different positions ($P_{\text{out}1}$, $P_{\text{out}2}$, and $P_{\text{out}3}$, respectively). All the autocorrelation traces were fitted to the autocorrelation of sech^2 pulse. While the autocorrelation traces of the intracavity pulses ($P_{\text{out}1}$ and $P_{\text{out}2}$) were well fit to the autocorrelation of sech^2 in overall range of the coarse cavity detuning, the autocorrelation traces of the pulse from BS1 ($P_{\text{out}3}$) did not fit well to the autocorrelation of sech^2 and serious temporal modulation in autocorrelation trace was observed. This temporal modulation was mainly observed in the negative cavity detuning, i.e. in the region of generating shorter pulses. Although there is some ambiguity, the intensity autocorrelation can be a useful tool to observe the temporal modulation of the pulse. The temporal modulation in the autocorrelation trace means the temporal modulation in the pulse profile. On account of properties of the interferometric addition of APM at the beam splitter, the low intensity part of the pulse could be highly transmitted than the high intensity part at the beam splitter. This effect can cause the temporal modulation of the pulse in the case of extracting an output through BS1.

In order to verify the fact that the interferometric addition at the beam splitter may cause the temporal modulation of mode-locked pulses and to understand the effect of the coarse cavity detuning on the temporal profile, the temporal shape and autocorrelation were calculated with various cavity detuning values with Eq. (6). Fig. 6 shows the variation of the

temporal profile and its autocorrelation experienced by the non-linear reflectance due to the interferometric nature with respect to the coarse cavity detuning. In the calculation, the reflectance of the beam splitter and the coupling loss were taken as 85% and 0.74, respectively, and the pulse width at each cavity detuning was taken from Fig. 3. The time delay due to the coarse cavity detuning was defined by $2\Delta L/c$. Fig. 6 shows the interferometric nature in APM induces the temporal modulation in the mode-locked pulse in the case of an output through BS1, and this temporal modulation can be reflected as a deviation of the intensity autocorrelation trace from sech^2 pulse shape. Although pulses were temporally modulated at the beam splitter, the calculation showed that the intracavity pulses could be temporally clean and short. It means that it is not appropriate to use the beam splitter as the output coupler. Our previous result [13] of 1.5 ps pulse width obtained from BS1 and the lower value of the time bandwidth product ($\Delta\nu\Delta\tau$) than the transform-limited value, 0.315, occurred mainly by the effect of this temporal modulation.

In some applications, clean pulses without any temporal modulation may be required. In this case, it is better not to obtain an output through the beam splitter at which the temporal modulation may occur due to the interferometric addition. To obtain a temporally clean pulse with higher output power than that of $P_{\text{out}2}$, the full mirror (M1), at which clean pulses were circulating, was replaced with an output coupler with the reflectance of 94%. The

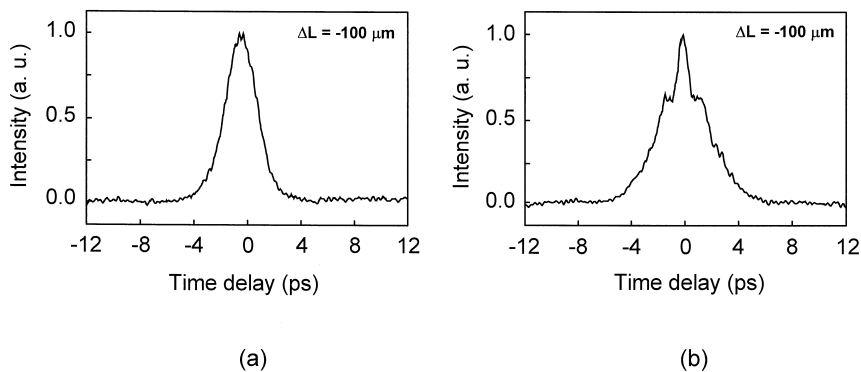


Fig. 7. Autocorrelation traces of an LD pumped, additive-pulse mode-locked Nd:YLF laser when generating shortest pulses with 94% output coupler. Autocorrelation from (a) 94% output coupler (M1) and (b) the beam splitter (BS1).

mode-locking was also maintained through the cavity detuning range of about 300 μm . The position generating the shortest pulse width and the broadest spectrum did not change from that of Fig. 3. The autocorrelation traces of the outputs at the cavity condition of shortest pulse generation through the mirror M1 and BS1 are shown in Fig. 7a,b, respectively. Although the temporal modulation was observed in Fig. 7b, no temporal modulation was observed in the autocorrelation in Fig. 7a from the output coupler, M1. When obtaining the shortest pulse width of 1.7 ps, the spectral width was measured 7.3 \AA , giving the time bandwidth product of 0.34. Consequently, the direct extraction of an output from the main cavity is necessary for the generation of transform-limited, clean pulses from an APM laser.

5. Conclusion

The characteristics of an LD-pumped APM Nd:YLF laser such as the pulse width, spectrum, and temporal modulation were investigated with respect to the coarse cavity detuning. From this investigation, the method to generate the shortest and clean pulses was studied in the APM laser. The peak of the output pulse spectrum was shifted to the short wavelength when decreasing the external cavity length. When the beam splitter commonly used to link the main and external cavities was utilized as an output coupler, the temporal modulation of the output pulse was observed from the autocorrelation trace, which also agreed with the calculation using an intensity-dependent reflectance. For the generation of short and clean from an APM laser, The direct extraction of an output from the main cavity proved to be

crucial and 1.7 ps pulses without any temporal modulation were obtained from the LD-pumped APM Nd:YLF laser.

Acknowledgements

This research was supported by the Agency for Defense Development, Korea, through the Center for Electro-Optics at the KAIST.

References

- [1] J. Goodberlet, J. Wang, J.G. Fujimoto, P.A. Schulz, *Optics Lett.* 14 (1989) 1125.
- [2] D.E. Spence, P.N. Kean, W. Sibbett, *Optics Lett.* 16 (1991) 42.
- [3] J. Goodberlet, J. Jacobson, J.G. Fujimoto, P.A. Schulz, T.Y. Fan, *Optics Lett.* 15 (1990) 504.
- [4] G.P.A. Malcolm, P.E. Curley, A.I. Ferguson, *Optics Lett.* 15 (1990) 1303.
- [5] F. Krausz, C. Spielmann, T. Brabec, E. Winter, A.J. Schmidt, *Optics Lett.* 15 (1990) 737.
- [6] E.P. Ippen, L.Y. Liu, H.A. Haus, *Optics Lett.* 15 (1990) 183.
- [7] M.N. Kong, J.K. Chee, J.M. Liu, *Optics Lett.* 16 (1991) 73.
- [8] X. Zhu, P.N. Kean, W. Sibbet, *IEEE J. Quantum Electron.* 25 (1989) 2445.
- [9] J. Herrmann, M. Muller, *J. Opt. Soc. Am. B.* 13 (1996) 1542.
- [10] H.A. Haus, J.G. Fujimoto, E.P. Ippen, *IEEE J. Quantum Electron.* 28 (1992) 2086.
- [11] J.K. Chee, J.M. Liu, M.N. Kong, *IEEE J. Quantum Electron.* 28 (1992) 700.
- [12] J. Mark, L.Y. Liu, K.L. Hall, H.A. Haus, E.P. Ippen, *Optics Lett.* 14 (1989) 48.
- [13] E.C. Kang, T.M. Jeong, J.M. Lee, C.H. Nam, *Jpn J. Appl. Phys.* 28 (1998) 700.
- [14] F.M. Mitschke, L.F. Mollenauer, *IEEE J. Quantum Electron.* 22 (1986) 2242.
- [15] H.A. Haus, U. Keller, W.H. Knox, *J. Opt. Soc. Am. B* 8 (1991) 1252.
- [16] E.P. Ippen, H.A. Haus, L.Y. Liu, *J. Opt. Soc. Am. B* 6 (1989) 1736.